Evaporatively controlled growth of salt trees

Rose Du and H. A. Stone*
Division of Applied Sciences, Harvard University, Cambridge, Massachusetts 02138
(Received 8 August 1995)

During the latter stages of the evaporation of ammonium chloride solutions, highly ramified salt structures, centimeters in height, are formed. In contrast with many, if not all, of the commonly discussed branched solidified objects (e.g., dendrites or diffusion-limited aggregation clusters), the porous nature of the salt trees leads to growth in a direction away from the material source owing to a coupling between capillarity and evaporation. A physical mechanism for the phenomenon is reported, growth as a function of external convection is studied and demonstrates growth directed opposite the convective flow, and a method for determining a fractal dimension of the three-dimensional trees is described.

PACS number(s): 61.43.Hv, 68.70.+w, 81.30.Mh, 91.60.−x

I. INTRODUCTION

Branched structures are observed in many areas of physics, material science, biology, and the earth sciences. Often the underlying, perhaps competing, physical processes responsible for the detailed microstructure can be identified. For example, in recent years there have been many studies of the common branched structures observed in electrochemical deposits [1], diffusion-limited aggregation (DLA) clusters [2], patterns from reactive dissolution of porous materials [3], dendrites generated during solidification processes [4], and crystalline aggregates precipitated in silica gels [5]. In all of these cases diffusion is the basic transport process [6], and fractal structures are common with growth occurring towards the material source when solidification is the operative mechanism.

Here we present experimental results, along with a mechanistic description, of the porous "treelike" structures that grow during the latter stages of the evaporation of ammonium chloride solutions. From the viewpoint of standard pattern formation studies, these structures are unusual since the coupling of evaporation and capillarity leads to growth in the direction opposite to the material source. Mineral deposits contain the necessary elements for this manner of precipitation and macroscopic growth. Consequently, the processes described here are relevant for a proper understanding of the surface coverings frequently observed (but not mechanistically described) on museum specimens and of the development of some surface features in wet limestone caves [7–9].

II. EXPERIMENTAL RESULTS

Ammonium chloride salt trees are formed by allowing a saturated aqueous solution of ammonium chloride to evaporate under normal laboratory conditions. The typical growth sequence is shown in Fig. 1. During the initial stages of evaporation, the growth of ammonium chloride dendrites produces a porous matrix of solid crystals with saturated fluid in the interstices. This porous network is referred to as a "mushy layer" and has been studied, for example, owing to its relevance to the solidification of binary alloys [10]. As evaporation continues, a thin crust of salt forms at the air-mush interface and small perturbations at the interface are generated owing to the underlying crystallization process. Provided the relative humidity is lower than about 50% and there is some background convection, the perturbations of the salt crust develop into highly branched treelike structures, which are typically a few centimeters in height as shown in Fig. 1(d).

We tried to perform these experiments with other salts (e.g., K_2CO_3) though only ammonium chloride developed into highly branched trees. However, Na_2SO_4 occasionally formed very small branched trees, which were rather fragile, and also grew opposite to the source location [11].

Porous microstructure. Scanning electron micrographs of the surface and interior of a branch clearly indicate that the salt structures are porous. Figure 2(a) shows the highly branched object that develops. A cross section of the base of a typical branch, shown in Fig. 2(b), illustrates the porous interior, which is likely representative of the exterior surface during growth. The interior pore sizes have approximate radii 30–300 μm. Treating the pores as capillary tubes and using the force balance $2\sigma/r \approx \rho g h$, where σ, r, ρ, g, and h denote, respectively, the interfacial tension, tube radius, fluid density, gravitational acceleration, and tree height, we can estimate the maximum structure sizes. Taking the representative values for saturated salt solutions $\sigma \approx 75$ dyn cm^{-1} and $\rho = 1.07$ g cm^{-3}, we obtain $h \approx 4.8$–48 cm. The lower limit is the order of magnitude of the typical laboratory grown trees. This result indicates that capillarity provides sufficient force to support the fluid at the tree extremities. Also, dye added at the base of a tree is observed to travel rapidly to all the branches. We note that, as the surface tension of salt solutions increases with an

*Author to whom correspondence should be addressed.

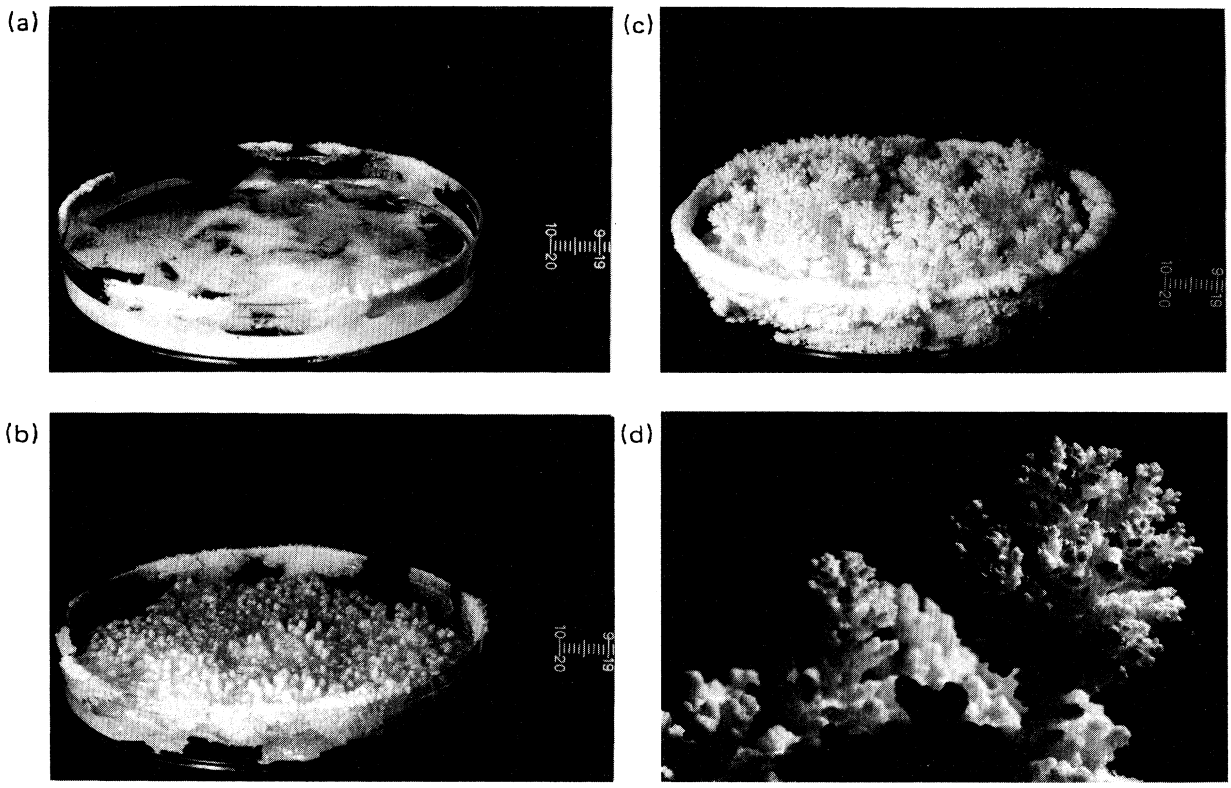

FIG. 1. Stages of growth of ammonium chloride salt trees. 50 ml of a saturated ammonium chloride solution, 26% NH_4Cl by weight, was placed in a 100×15 mm^2 plastic Petri dish and allowed to evaporate under typical laboratory conditions [(28 ± 2)% relative humidity, $24 \pm 2\,^{\circ}$C; the relative humidity of the saturated ammonium chloride solution is 79%]. (a) A typical initial stage of evaporation showing a porous matrix, or mushy layer, of ammonium chloride dendrites. A scale with millimeter graduations is shown at right. (b) Intermediate stage of evaporation, approximately 7 h after the initial stage: thin crust develops small perturbations. (c) Final stage of evaporation, approximately 10 h after (b), showing highly branched salt trees, the largest of which is approximately 1.3 cm in height. (d) A close-up of a typical tree. We note that in the British Natural History Museum there is a sample of NH_4Cl, the mineral sal ammoniac, which has the form of these small trees.

increase in salt concentration, a surface-tension-driven flow may aid transport to regions of local evaporation and growth (e.g., [12]). However, this transport mechanism is less likely to be important for the highly contorted surfaces with large surface area shown in Fig. 2. Overall, the porous surface, wetting characteristics of the aqueous solution, strong capillarity, and the observed growth at the tips of the branches suggest the presence of a thin film of fluid along the surface of the trees. Evaporation from the film produces a supersaturated solution which promotes crystallization.

Developing a quantitative description and model is difficult since perturbations occur on two different length scales: the diameter of the base of a typical branch is several hundred micrometers and the perturbations which form the porous interior of a tree have dimensions smaller than ten micrometers. The growth of the microscopic porous network can be described qualitatively by a model similar to that used for describing the solidification of binary melts [4,13]. In a film of solution along a solid surface there is a concentration gradient of solute due to evaporation of water from the fluid-air interface and crystallization along the fluid-solid interface. Perturbations of the solid surface thus invade an environment of higher salt concentration, which serves to promote further crystallization, resulting in unstable perturbations. Perturbations of sufficiently short wavelength, however, are stabilized by the increase in surface energy [4,13]. The irregular structure of the porous interior [Fig. 2(b)] is consistent with the idea that a wide range of disturbances of the solid surface are unstable in the presence of the evaporatively generated salt gradient.

Effect of convection. The macroscopic features of the trees are affected by convection and humidity. The qualitative effects of convection are studied by varying the distance of a solution-filled Petri dish from a small fan. A convectively grown colony of trees is shown in Fig. 3 and we note that the tree growth is toward the convective source. Stronger convection (typically velocities larger than 10–20 cm s^{-1}) produces finer branches, cylindrically shaped formations, more closely spaced trees, and preferential growth at the leading edge of the Petri dish. Sparse growth in the middle of the dish is a result of the shielding by the edge of the dish. To eliminate convective influ-

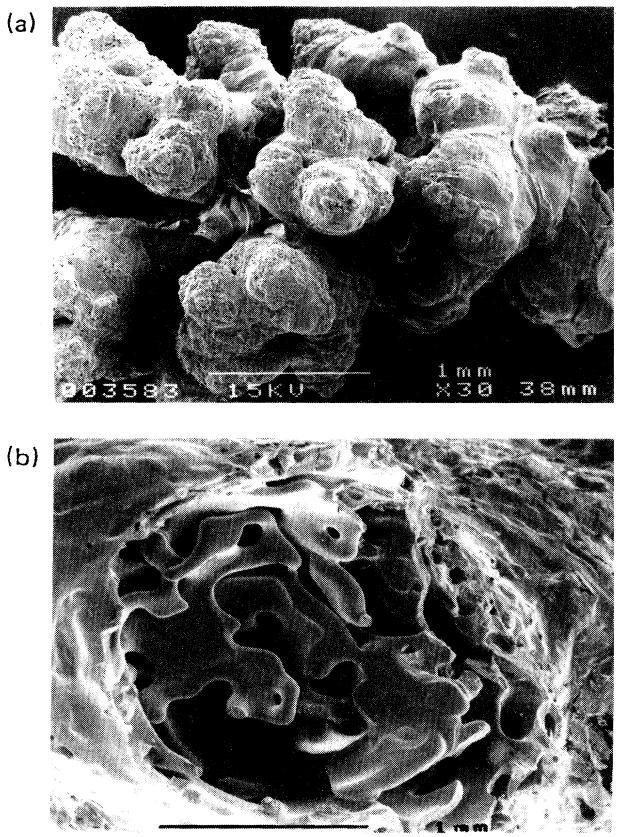

FIG. 2. Scanning electron micrographs of typical ammonium chloride salt trees. (a) A branch of a dried tree approximately 3 mm in length. The small pores covering the surface appear to be a consequence of the last stages of evaporation and/or the preparation for viewing in the scanning electron microscope. (b) Cross section of the base of a typical dried tree showing the porous interior. This structure appears to be representative of the porous surface during the growth of the tree. Observations suggest the presence of a thin fluid film maintained by capillarity on the porous surface of the tree.

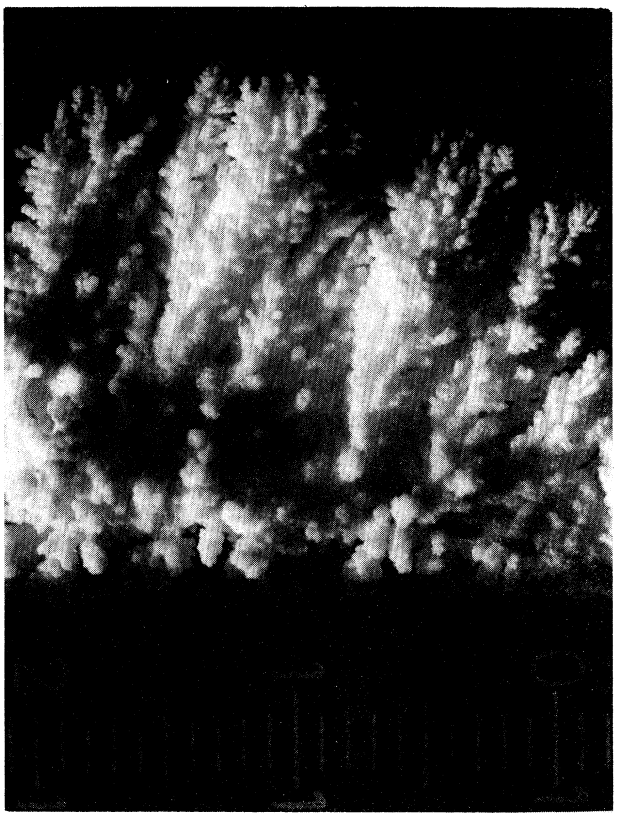

FIG. 3. A top view of ammonium chloride salt trees grown at (36±1)% relative humidity and 25±0.5 °C. A fan is located at the top of the figure and creates a unidirectional convective flow with speeds about 180 cm s^{-1} in the neighborhood of the edge of the Petri dish. The scale shown has millimeter graduations. Convection produces finely branched, cylindrically shaped trees, which are closely spaced and oriented toward the convective source.

ences, experiments were performed in a closed aquarium using other salts ($CaCl_2$ and K_2CO_3) to control the ambient relative humidity in the range [(30–50)±3]%. The absence of convection resulted in small stublike perturbations without substantial growth or branching.

The experimental observations, which demonstrate the strong influence of convection on the branching characteristics, suggest that vapor phase transport of water plays a dominant role in the growth process. Thus we expect that, given convection with velocity U, macroscopic tree growth is controlled by a boundary layer of air, with thickness δ proportional to $U^{-1/2}$, across which water molecules diffuse. Such a simple model for macroscopic instabilities of a porous surface shows that all perturbations are linearly unstable because the perturbations increase the water flux (and hence crystallization) from surfaces closer to the edge of the boundary layer. Physically, we expect that diffusion parallel to the surface becomes important for shorter wavelengths, which in a nonlinear stability analysis may produce stabilization and hence yield a preferred structure size, though we have been unable to carry out the details of such an analysis. Qualitatively this simple explanation is in agreement with the observation that the branching increases (and tree spacing decreases; Fig 3) as the external convection is increased. Stabilization is perhaps possible by resistance of flow through the porous matrix or slow liquid phase diffusion, though the earlier estimates of strong capillary effects suggest these influences to be less important.

Measurement of a fractal dimension. We have characterized the structure of the salt trees by measuring their fractal dimensions for varying degrees of forced convection. The experimental determination of a fractal dimension of a three-dimensional object is nontrivial [14]; the method used in this work is straightforward, but destroys the sample. We define the fractal dimension d in terms of the mass m of a branch, and the length l of a branch, or part of a branch, in the direction of growth, according to

$$m = k\, l^d , \tag{2.1}$$

where k is a constant. After measuring the mass and

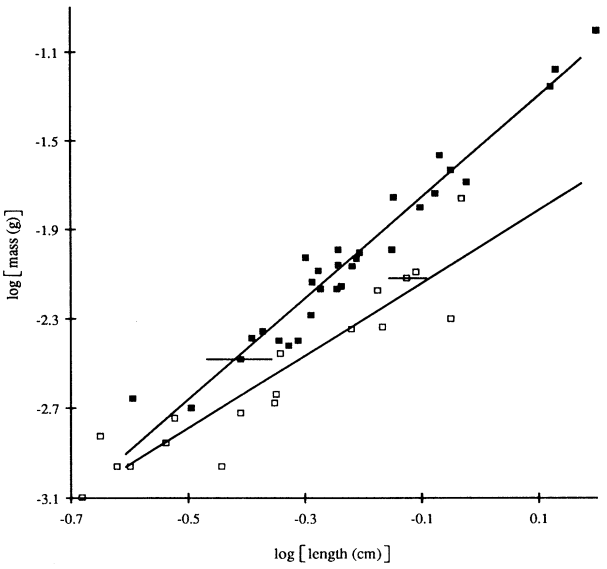

FIG. 4. Mass of a branch of an ammonium chloride salt tree as a function of the branch length (logarithms are base 10). Lines shown are least squares fit of the data. (a) Trees grown under relatively weak convection (velocity < 20 cm s^{-1}) in the middle of the Petri dish exhibit fractal dimensions $d > 2$; least squares correlation $r = 0.97$, slope $= 2.26 \pm 0.10$ (■). (b) Trees grown under stronger convection (velocity < 300 cm s^{-1}) on the edge of the Petri dish exhibit $d < 2$; least squares correlation $r = 0.93$, slope $= 1.61 \pm 0.16$ (□).

length of a tree (branch), it is broken into subbranches each of which is measured by repeating the above procedures. Typical results for mass as a function of length are given in Fig. 4 where we compare data for trees that grow exposed to different degrees of external convection.

A fractal growth response is observed over a decade in salt structure size. Under relatively weak convection where substantial tree growth occurs away from the leading edge of the container (Fig. 1), the fractal dimension varies in the range $2.1 \pm 0.2 < d < 2.4 \pm 0.2$. There does not appear to be any regular variation of these values as a function of increased distance from the convective source. Trees grown along the front edge of the Petri dish are affected by external convection, as shown in Fig. 3, and are characterized by a fractal dimension in the range $1.6 \pm 0.2 < d < 1.8 \pm 0.2$. In this case a dimension $d < 2$ is expected since the trees grown under stronger convective conditions develop nearly aligned with the direction of the external flow and are nearly cylindrical in overall shape. Comparing the two ranges of dimension values, it appears likely that there is a continuous variation of the fractal dimension as a function of the strength of the external flow. Since the fractal dimension indicates the directionality of growth, the measured dimension (or simply the characteristic shape, cylindrical versus spherical) has the potential to indicate the presence and strength of the convective effects during this type of coupled evaporative-capillary growth.

III. CONCLUSIONS

The ammonium chloride salt trees described in this paper represent a type of nonequilibrium pattern formation and fractal mineral growth process in which the direction of growth is away from the material source. The trees appear to be related, in both structure and ambient growth conditions, to some of the calcite and aragonite deposits that frequently decorate limestone caves in the form of small treelike structures on the sides of stalactites and the cave walls [8,15]. Similar branched structures are observed in a variety of surface coverings found in mineral deposits and on display in museums.

ACKNOWLEDGMENTS

We thank C. Hayzelden for performing many of the SEMS, A. Dionne for his photography, P. Evesque for suggesting the method for determining the fractal dimension of the trees, and G. Worster for encouragement to do experiments with ammonium chloride solutions that eventually led to the observations described here. Discussions with M. Aziz, H. Emmons, C. Francis, F. Spaepen, S. Strogatz, and L. Trefethen, as well as many other members of the Harvard community, are gratefully acknowledged. This work was supported by NSF (CTS-8957043 to H.A.S.) R.D. acknowledges the Ford Foundation for partial support.

[1] R. M. Brady and R. C. Ball, Nature **309**, 225 (1984).
[2] H. E. Stanley, A. Bunde, S. Havlin, J. Lee, E. Roman, and S. Schwarzer, Physica A **168**, 23 (1990).
[3] G. Daccord and L. Lenormand, Nature **325**, 41 (1987).
[4] W. W. Mullins and R. F. Sekerka, J. Appl. Phys. **35**, 444 (1964); J. S. Langer, Rev. Mod. Phys. **52**, 1 (1980).
[5] T. Baird, P. S. Braterman, P. Chen, J. M. Garcia-Ruiz, R. D. Peacock, and A. Reid, Mater. Res. Bull. **27**, 1031 (1992).
[6] E. Ben-Jacob and P. Garik, Nature **343**, 523 (1990).
[7] W. B. White, in *The Science of Speleology,* edited by T. D. Ford and C. H. D. Cullingford (Academic Press, London, 1976), pp. 267–327.
[8] D. Ford and P. Williams, *Karst Geomorphology and Hydrology* (Chapman & Hall, London, 1989).
[9] L. C. Huff, J. Geol. **40**, 641 (1948).
[10] H. Huppert, J. Fluid Mech. **212**, 209 (1990).
[11] During the course of this work it was brought to our attention that many museum and/or toy stores sell a demonstration under the trade name *Magic Tree*® that exhibits evaporatively driven tree growth; no information regarding the chemical constituents is given, though the fragile branched objects appeared similar in structure to the Na_2SO_4 trees.
[12] G. W. Sears, J. Chem. Phys. **26**, 1549 (1957).
[13] P. G. Shewmon, Trans. Metall. Soc. AIME **233**, 736 (1965); D. P. Woodruff, *The Solid-Liquid Interface* (Cambridge University Press, London, 1973).
[14] R. Lenormand, A. Soucémarianadin, E. Touboul, and G. Daccord, Phys. Rev. A **36**, 1855 (1987).
[15] A. W. Wells, Stud. Speleol. **2**, 129 (1971).

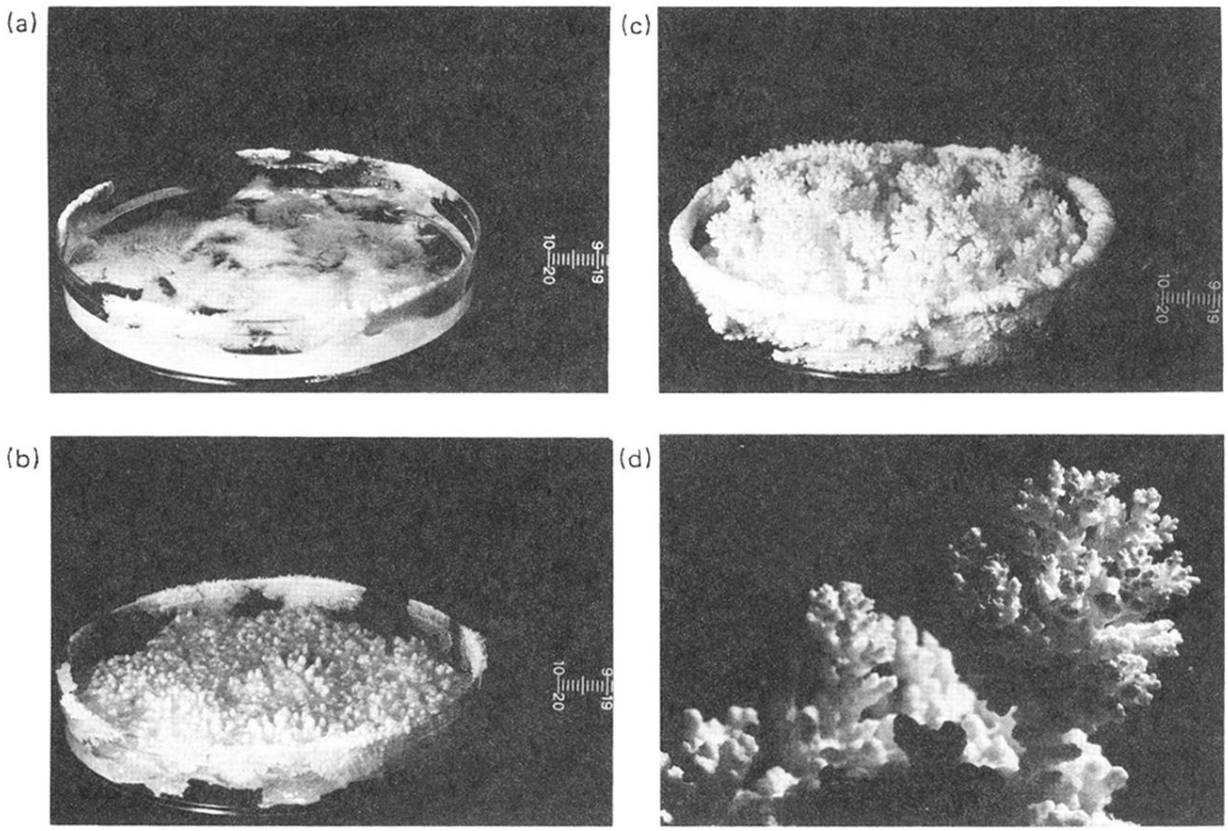

FIG. 1. Stages of growth of ammonium chloride salt trees. 50 ml of a saturated ammonium chloride solution, 26% NH_4Cl by weight, was placed in a 100×15 mm^2 plastic Petri dish and allowed to evaporate under typical laboratory conditions [(28 ± 2)% relative humidity, $24 \pm 2\,^{\circ}C$; the relative humidity of the saturated ammonium chloride solution is 79%]. (a) A typical initial stage of evaporation showing a porous matrix, or mushy layer, of ammonium chloride dendrites. A scale with millimeter graduations is shown at right. (b) Intermediate stage of evaporation, approximately 7 h after the initial stage: thin crust develops small perturbations. (c) Final stage of evaporation, approximately 10 h after (b), showing highly branched salt trees, the largest of which is approximately 1.3 cm in height. (d) A close-up of a typical tree. We note that in the British Natural History Museum there is a sample of NH_4Cl, the mineral sal ammoniac, which has the form of these small trees.

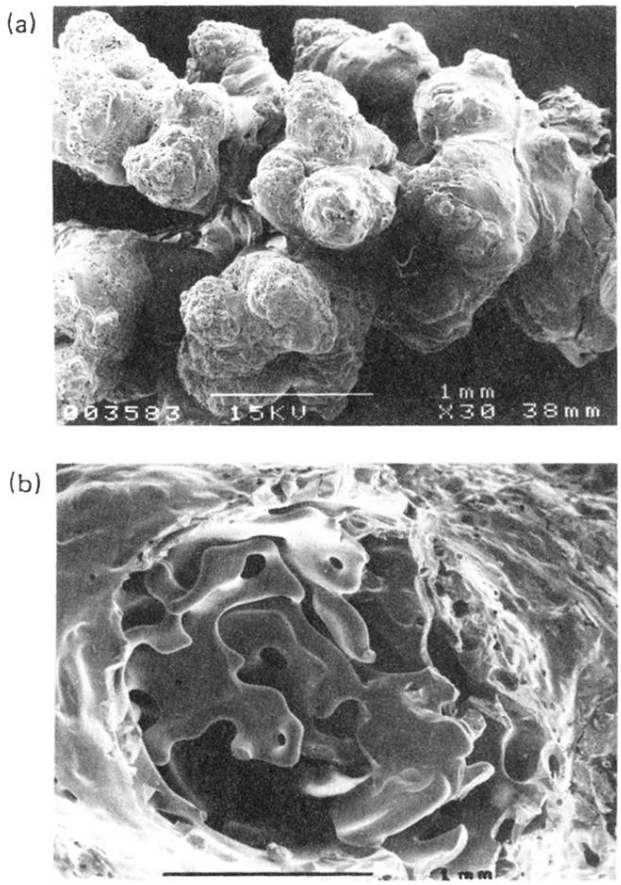

FIG. 2. Scanning electron micrographs of typical ammonium chloride salt trees. (a) A branch of a dried tree approximately 3 mm in length. The small pores covering the surface appear to be a consequence of the last stages of evaporation and/or the preparation for viewing in the scanning electron microscope. (b) Cross section of the base of a typical dried tree showing the porous interior. This structure appears to be representative of the porous surface during the growth of the tree. Observations suggest the presence of a thin fluid film maintained by capillarity on the porous surface of the tree.

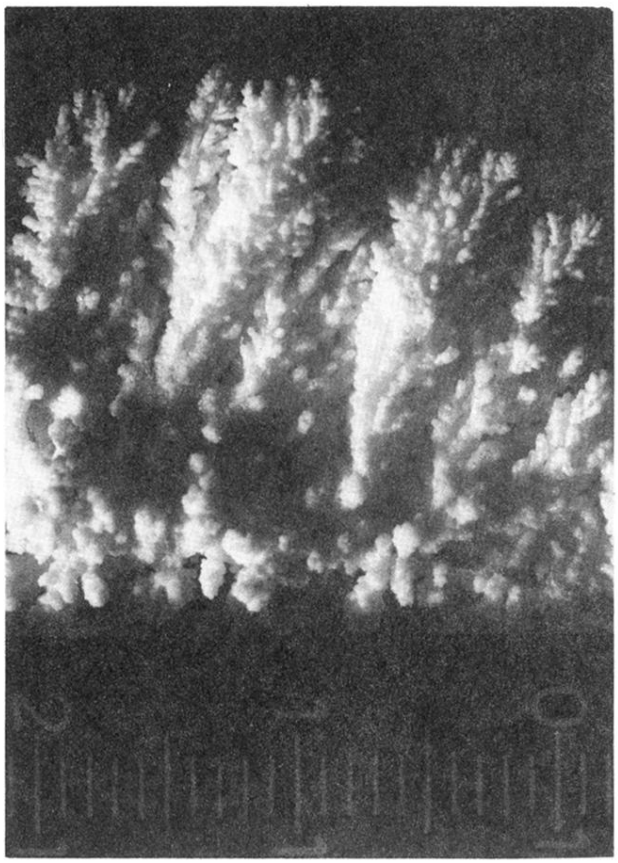

FIG. 3. A top view of ammonium chloride salt trees grown at (36±1)% relative humidity and 25±0.5 °C. A fan is located at the top of the figure and creates a unidirectional convective flow with speeds about 180 $\mathrm{cm\,s^{-1}}$ in the neighborhood of the edge of the Petri dish. The scale shown has millimeter graduations. Convection produces finely branched, cylindrically shaped trees, which are closely spaced and oriented toward the convective source.